



# Phase equilibria and magnetism in the Mo–Si–U system

Peter Rogl<sup>a,\*</sup>, Tristan Le Bihan<sup>a,b</sup>, Henri Noël<sup>b</sup>

<sup>a</sup> Institut für Physikalische Chemie der Universität Wien, Währingerstraße 42, A-1090 Vienna, Austria

<sup>b</sup> Laboratoire de Chimie du Solide et Inorganique Moléculaire, Université de Rennes I, U.M.R. C.N.R.S. 6511, Avenue du Général Leclerc, F-35042 Rennes cedex, France

Received 17 July 2000; accepted 7 October 2000

## Abstract

Phase equilibria in the system Mo–Si–U were established at 1400°C for the region less than 60 at.% U and at 850°C for the region less than 70 at.% Si by optical microscopy, EMPA and X-ray diffraction. Three ternary compounds were observed and characterised by X-ray powder or single-crystal data refinement: (1) stoichiometric  $U_2Mo_3Si_4$  ( $U_2Mo_3Si_4$ -type); (2)  $U(Mo_{1-x}Si_x)_2$  (MgZn<sub>2</sub>-type) extending at 1400°C from  $U(Mo_{0.62}Si_{0.38})_2$  to  $U(Mo_{0.75}Si_{0.25})_2$  but with a small field of existence at 850°C around  $U(Mo_{0.68}Si_{0.32})_2$  and (3)  $U_4Mo(Mo_xSi_{1-x})_1Si_2$  (ordered structure variant of  $W_5Si_3$ -type) extending at 850°C from  $x = 0$  to  $x = 0.33$ . The magnetic behaviour of the three compounds is characterised by temperature independent paramagnetism. © 2001 Elsevier Science B.V. All rights reserved.

## 1. Introduction

In continuation of our systematic studies [1–4] of strong electron correlations in higher order intermetallics, we presently focus on the constitution, the structural chemistry and in particular on the possible occurrence of co-operative magnetism and/or superconductivity depending on the 5f-hybridisation in ternary uranium base alloy systems with 4d-metals and silicon. Despite phase equilibria have not been evaluated in detail for the Mo–Si–U ternary, early reports mentioned the existence and crystal structure of two ternary compounds:  $U_2Mo_3Si_4$  with a unique structure type [5] and  $U(Mo_{0.62}Si_{0.38})_2$  with the MgZn<sub>2</sub>-type [6]. Single crystal X-ray refinements [7,8] confirmed symmetry and structure type for both these compounds. For  $U(Mo_{0.62}Si_{0.38})_2$  a partial random occupation of Mo and Si atoms in the (2a) and (6h) sites of space group  $P6_3/mmc$  was established [7]. Recent studies [9,10] of the phase equilibria in the uranium-rich part of the diagram

at 850°C confirmed the existence of  $U_2Mo_3Si_4$ , but in addition claimed the formation of two further ternary compounds: ‘ $U_3MoSi_2$ ’ and ‘ $U_4MoSi_3$ ’, the crystal structures of which are still unaccounted for. A peritectic mode of formation was proposed for ‘ $U_3MoSi_2$ ’ according to the reaction:  $L + ‘U_4MoSi_3’ + U_2Mo_3Si_4 \rightleftharpoons ‘U_3MoSi_2’$  [9,10].

In order to provide details on the phase equilibria, the present paper deals with the phase relations in the complete isothermal section of the ternary, with the crystal structure of the observed ternary compounds as well as with their magnetic behaviour in the temperature range 1.4–300 K and in fields up to 6 T. As far as the phase equilibria and compatibility of  $U_3Si_2$  with Mo-metal are concerned, the research reported herein is related to low-enriched uranium (LEU) proliferation resistant reactor fuel systems [11,12].

## 2. Experimental

Samples usually were of a total weight of 1 g and were prepared by argon-arc or high frequency levitation melting. Platelets of depleted uranium (claimed purity of 99.9% by E. Merck, Darmstadt, D), pieces of 6 N-silicon

\* Corresponding author. Tel.: +43-1 4277 52456; fax: +43-1 4277 9524.

E-mail address: peter.franz.rogl@univie.ac.at (P. Rogl).

(Alfa Ventron, Karlsruhe, D) and precompacted powders of molybdenum (99.9%, Metallwerk Plansee, Austria) were used as starting materials. The U-platelets were surface cleaned in diluted  $\text{HNO}_3$  prior to melting. The samples were remelted several times for homogeneity and weight losses were checked to be altogether less than 0.5 mass%. For the alloys with a uranium content less than 40 at.% U, a part of each button was annealed at 1400°C for 200 h on a W-substrate in a high-vacuum furnace with a W-sheet metal thyristor controlled heating system under a dynamic vacuum better than  $10^{-4}$  Pa. After heat treatment the samples were cooled by switching off the power to the furnace. A part of each of the U-rich alloys was contained within a small alumina crucible, sealed in evacuated silica tubes and heat treated at 850°C for 250 h and finally quenched by submerging the capsules in cold water. Further details of sample preparation, of the X-ray techniques used (including quantitative Rietveld analyses employing the Fullprof program [13]) as well as a general description of the magnetic measurements (SQUID-magnetometer) may be found in our preceding publication on binary uranium silicides [14] or on the ternary system Nb–Si–U [4].

X-ray intensity data for a single-crystal of  $\text{U}_4\text{Mo}(\text{Mo}_{0.33}\text{Si}_{0.67})_2\text{Si}_2$  were collected for a hemisphere in 352 images (total exposure time 345 min) on a four-circle Nonius Kappa diffractometer equipped with a CCD area detector employing graphite monochromated  $\text{MoK}\alpha$ -radiation ( $\lambda = 0.071073$  nm). Orientation matrix and unit cell parameters were derived from the first ten data frames using the program DENZO [15]. Absorption correction was taken from program SORTAV [15] ( $\mu = 107.8$   $\text{mm}^{-1}$ ). The structure was refined with the aid of the SHELXS-97 program [16]. The single-crystal platelet with small dimensions ( $8 \times 20 \times 30$   $\mu\text{m}^3$ ) was obtained by mechanical fragmentation of an alloy  $\text{U}_3\text{MoSi}_2$ , which after arc-melting was annealed in an alumina crucible under argon at 1150°C for 6 h and slowly cooled to room temperature.

Microstructures were inspected by optical microscopy on SiC-ground and 1/4  $\mu\text{m}$  diamond paste polished surfaces, etched by a mixture of 1  $\text{cm}^3$  HF + 5  $\text{cm}^3$   $\text{H}_2\text{O}_2$  in 94  $\text{cm}^3$  of  $\text{H}_2\text{O}$ . A CAMEBAX SX50 wavelength dispersive X-ray microanalyser (EMPA-XMA) was used for proper identification of the phases and precipitates. Measurements were performed at an acceleration voltage of 15 kV at 20 nA sample current and employing spectrometer crystals such as PET for the U– $\text{M}\alpha$ , Mo– $\text{L}\alpha$  and TAP for the Si– $\text{K}\alpha$  radiation. For quantitative analyses the ZAF correction program was employed [17] comparing the characteristic radiation of the elements from the alloy with that obtained from  $\text{UO}_2$ , elemental Mo and  $\text{SiO}_2$  as reference materials. The sum of mass% for the individual elemental measurements were in all alloys investigated within  $(100 \pm 0.8)$  mass%.

### 3. Results and discussion

#### 3.1. The binary boundary systems

The binary boundary systems Mo–U and Mo–Si were accepted from a critical assessment of binary alloy phase diagrams by Massalski [18]. The U–Si system used herein is the version established in a recent reinvestigation by the authors [14]. The uranium-rich part of the diagram up to 4 at.% Si is taken from [11]. Crystallographic data of the binary boundary phases can be found in Massalski [18] in combination with Villars [19]. Information on the magnetic behaviour of the binary uranium silicides is provided in [14]. The magnetic behaviour intrinsic to the uranium–molybdenum binary system is compiled in [20].

#### 3.2. The ternary system Mo–U–Si

##### 3.2.1. Phase relations at 1400°C

Phase relations within the Mo–U–Si ternary system were established for the isothermal section at 1400°C for uranium concentrations smaller than 70 at.% (Fig. 1). Two ternary compounds were revealed:  $\text{U}_2\text{Mo}_3\text{Si}_4$  [5,8] with the  $\text{U}_2\text{Mo}_3\text{Si}_4$ -type [8] and the ternary MgZn<sub>2</sub>-type Laves phase  $\text{U}(\text{Mo}_{1-x}\text{Si}_x)_2$  [6,7]. From optical microscopy and variation of lattice parameters  $\text{U}_2\text{Mo}_3\text{Si}_4$  is observed at its stoichiometric composition, whilst the Laves phase extends at 1400°C over a significantly wide homogeneous region, i.e. from  $\text{U}(\text{Mo}_{0.62}\text{Si}_{0.38})_2$  to  $\text{U}(\text{Mo}_{0.75}\text{Si}_{0.25})_2$ : the narrow range of existence at a stoichiometric content of uranium clearly indicates a partially random substitution of Mo/Si in the (6h) and the (2a) sites of space group  $\text{P6}_3/\text{mmc}$  (see below).

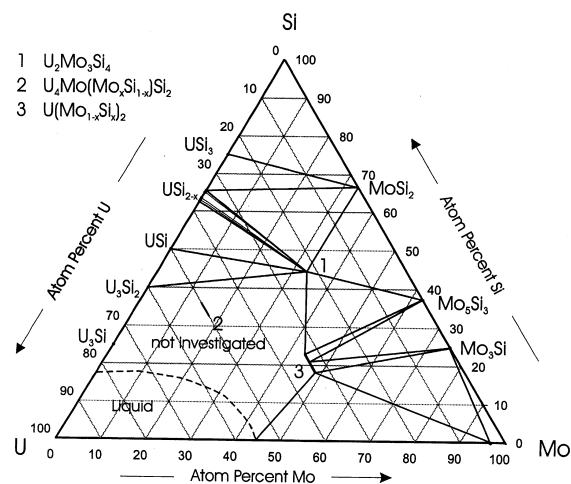


Fig. 1. Partial isothermal section at 1400°C of the Mo–Si–U system for U-concentrations < 70 at.%.

Table 1  
Crystallographic data of ternary alloys U–Mo–Si annealed at 1400°C

Nominal composition (in at.%)			Phase analysis	Space group	Prototype	Lattice parameters (nm)		
U	Mo	Si				<i>a</i>	<i>b</i>	<i>c</i>
17	16	67	$\alpha\text{MoSi}_2$	I4/mmm	MoSi <sub>2</sub>	0.32035(4)	–	0.78447(16)
			USi <sub>3</sub>	Pm $\bar{3}$ m	Cu <sub>3</sub> Au	0.40576(9)	–	–
			USi <sub>1.88</sub>	I4 <sub>1</sub> /amd	def.ThSi <sub>2</sub>	0.39411(7)	–	1.3747(6)
25	20	55	$\alpha\text{MoSi}_2$	I4/mmm	MoSi <sub>2</sub>	0.32031(3)	–	0.78415(35)
			U <sub>3</sub> Si <sub>5</sub> (o2)	Pmmm(?)	dist.AlB <sub>2</sub>	0.3892(3)	0.6740(6)	0.4027(4)
			U <sub>2</sub> Mo <sub>3</sub> Si <sub>4</sub>	P2 <sub>1</sub> /c	U <sub>2</sub> Mo <sub>3</sub> Si <sub>4</sub>	0.6874(5)	0.6883(4) <sup>a</sup>	0.6761(5)
35	10	55	U <sub>3</sub> Si <sub>5</sub>	P6/mmm	def. AlB <sub>2</sub>	0.38488(7)	–	0.40696(10)
			USi	Pnma	FeB	0.56618(11)	0.76495(25)	0.39077(3)
			U <sub>2</sub> Mo <sub>3</sub> Si <sub>4</sub>	P2 <sub>1</sub> /c	U <sub>2</sub> Mo <sub>3</sub> Si <sub>4</sub>	Traces	–	–
10	40	50	$\alpha\text{MoSi}_2$	I4/mmm	MoSi <sub>2</sub>	0.32062(2)	–	0.78481(22)
			Mo <sub>5</sub> Si <sub>3</sub>	I4/mcm	W <sub>5</sub> Si <sub>3</sub>	0.96524(11)	–	0.48877(4)
			U <sub>2</sub> Mo <sub>3</sub> Si <sub>4</sub>	P2 <sub>1</sub> /c	U <sub>2</sub> Mo <sub>3</sub> Si <sub>4</sub>	Traces	–	–
35	20	45	USi	Pnma	FeB	0.56624(10)	0.76500(20)	0.39070(4)
			U <sub>3</sub> Si <sub>2</sub>	P4/mbm	U <sub>3</sub> Si <sub>2</sub>	0.73325(5)	–	0.38975(5)
			U <sub>2</sub> Mo <sub>3</sub> Si <sub>4</sub>	P2 <sub>1</sub> /c	U <sub>2</sub> Mo <sub>3</sub> Si <sub>4</sub>	Traces	–	–
22	33	45	U <sub>2</sub> Mo <sub>3</sub> Si <sub>4</sub>	P2 <sub>1</sub> /c	U <sub>2</sub> Mo <sub>3</sub> Si <sub>4</sub>	0.6876(3)	0.6883(1) <sup>b</sup>	0.6760(3)
15	50	35	Mo <sub>5</sub> Si <sub>3</sub>	I4/mcm	W <sub>5</sub> Si <sub>3</sub>	0.96520(10)	–	0.49152(4)
			U <sub>2</sub> Mo <sub>3</sub> Si <sub>4</sub>	P2 <sub>1</sub> /c	U <sub>2</sub> Mo <sub>3</sub> Si <sub>4</sub>	Traces	–	–
			U(Mo <sub>1-x</sub> Si <sub>x</sub> ) <sub>2</sub>	P6 <sub>3</sub> /mmc	MgZn <sub>2</sub>	0.53672(6)	–	0.85552(19)
10	60	30	Mo <sub>5</sub> Si <sub>3</sub>	I4/mcm	W <sub>5</sub> Si <sub>3</sub>	0.96493(5)	–	0.49080(4)
			Mo <sub>3</sub> Si	Pm $\bar{3}$ n	Cr <sub>3</sub> Si	0.48886(7)	–	–
			U(Mo <sub>1-x</sub> Si <sub>x</sub> ) <sub>2</sub>	P6 <sub>3</sub> /mmc	MgZn <sub>2</sub>	0.53688(9)	–	0.85611(12)
33	42	25	UMo <sub>1.25</sub> Si <sub>0.75</sub>	P6 <sub>3</sub> /mmc	MgZn <sub>2</sub>	0.53730(5)	–	0.85334(9)
33	50	17	UMo <sub>1.5</sub> Si <sub>0.5</sub>	P6 <sub>3</sub> /mmc	MgZn <sub>2</sub>	0.53735(7)	–	0.85958(9)
25	55	20	Mo <sub>3</sub> Si	Pm $\bar{3}$ n	Cr <sub>3</sub> Si	0.48895(5)	–	–
			(Mo)	Im $\bar{3}$ m	W	0.31430(7)	–	–
			U(Mo <sub>1-x</sub> Si <sub>x</sub> ) <sub>2</sub>	P6 <sub>3</sub> /mmc	MgZn <sub>2</sub>	0.53539(8)	–	0.85521(14)
25	60	15	Mo <sub>3</sub> Si	Pm $\bar{3}$ n	Cr <sub>3</sub> Si	0.48863(10)	–	–
			(Mo)	Im $\bar{3}$ m	W	0.31477(4)	–	–
			U(Mo <sub>1-x</sub> Si <sub>x</sub> ) <sub>2</sub>	P6 <sub>3</sub> /mmc	MgZn <sub>2</sub>	0.53683(5)	–	0.85791(10)

<sup>a</sup>  $\beta = 109.80(4)^\circ$ .

<sup>b</sup>  $\beta = 109.79(2)^\circ$ .

As most of the surrounding phases engage in two-phase equilibria with U<sub>2</sub>Mo<sub>3</sub>Si<sub>4</sub>, a relatively high thermodynamic stability of this ternary compound is inferred. Phase analysis and lattice parameters of a series of ternary alloys are listed in Table 1. Lattice parameters and unit cell dimensions of the boundary phases obtained from ternary multiphase alloys annealed at 1400°C compare well with those of the pure binary phases as given in [18,19]. This result supports the conclusion for negligible mutual solid solubility among binary uranium and molybdenum silicides (see also Fig. 1). This is particularly true for U<sub>3</sub>Si<sub>2</sub> which showed at 1400°C insignificant solubility for molybdenum (<0.5 at.% Mo, from EMPA). Silicon-poor alloys with less

than 20 at.% Si at 1400°C appeared partially molten. Phase equilibria for this part of the diagram have been evaluated on samples annealed at 850°C (see below).

### 3.2.2. Phase relations at 850°C

The evaluation of a series of alloys, all with a uranium content of 50 at.% U (for listing and results of analysis, see Table 2), in as-cast condition as well as after anneal at 850°C, indeed revealed the existence of a new ternary compound, however, with a small homogeneous range extending at 850°C from U<sub>4</sub>MoSi<sub>3</sub> to U<sub>4</sub>Mo<sub>1.3</sub>Si<sub>2.7</sub> ('U<sub>3</sub>MoSi<sub>2</sub>'). At 850°C the new phase at U<sub>49.8</sub>Mo<sub>12.8</sub>Si<sub>37.4</sub> (U<sub>4</sub>MoSi<sub>3</sub>) was observed in equilibrium with U<sub>3</sub>Si<sub>2</sub> (U<sub>59.4</sub>Mo<sub>0.1</sub>Si<sub>40.5</sub>) and with U<sub>2</sub>Mo<sub>3</sub>Si<sub>4</sub> (U<sub>23.3</sub>Mo<sub>32.5</sub>Si<sub>44.2</sub>).

Table 2  
Crystallographic and EMPA data of ternary alloys U–Mo–Si, as-cast and/or annealed at 850°C

Nominal composition (at.%)		Heat treatment	X-ray phase analysis	Space group	Prototype	Lattice parameters (nm)			Results of EMPA (at.%)			
U	Mo					Si	a	b	c	U	Mo	Si
33	37 <sup>a</sup>	850°C	U(Mo <sub>1-x</sub> Si <sub>x</sub> ) <sub>2</sub> U <sub>2</sub> Mo <sub>3</sub> Si <sub>4</sub>	P6 <sub>3</sub> /mmc P2 <sub>1</sub> /c	MgZn <sub>2</sub> U <sub>2</sub> Mo <sub>3</sub> Si <sub>4</sub>				33.8 23.3	43.9 34.6	22.3 42.1	
33	43	as-cast 850°C	U(Mo <sub>1-x</sub> Si <sub>x</sub> ) <sub>2</sub> U(Mo <sub>1-x</sub> Si <sub>x</sub> ) <sub>2</sub>	P6 <sub>3</sub> /mmc P6 <sub>3</sub> /mmc	MgZn <sub>2</sub> MgZn <sub>2</sub>	0.53658(7) 0.53663(4)	0.86103(21) 0.85417(19)					
33	46	850°C	U(Mo <sub>1-x</sub> Si <sub>x</sub> ) <sub>2</sub>	P6 <sub>3</sub> /mmc	MgZn <sub>2</sub>	0.53636(4)	0.85813(15)					
33	49 <sup>b</sup>	as-cast 850°C	U(Mo <sub>1-x</sub> Si <sub>x</sub> ) <sub>2</sub> U(Mo <sub>1-x</sub> Si <sub>x</sub> ) <sub>2</sub>	P6 <sub>3</sub> /mmc P6 <sub>3</sub> /mmc	MgZn <sub>2</sub> MgZn <sub>2</sub>	0.53584(3) 0.53670(10)	0.85560(14) 0.85901(18)					
33	56	850°C	U(Mo <sub>1-x</sub> Si <sub>x</sub> ) <sub>2</sub> (Mo) γ-(U <sub>1</sub> Mo)	P6 <sub>3</sub> /mmc Im $\bar{3}$ m Im $\bar{3}$ m	MgZn <sub>2</sub> W W				33.9 1.5 61.8	46.4 97.7 38.1	19.7 0.8 0.1	
51	6	850°C	U <sub>3</sub> Si <sub>2</sub> Fine eutectic structure	P4/mbm	U <sub>3</sub> Si <sub>2</sub>	0.73325(5)	0.38975(5)		59.7 45.1	0.3 13.4	40.0 41.5	
50	12.5	as-cast	U <sub>3</sub> Si <sub>2</sub> Fine eutectic structure	P4/mbm	U <sub>3</sub> Si <sub>2</sub>				57.6 76	1.6 10	40.8 14	
		850°C	U <sub>4</sub> MoSi <sub>3</sub> U <sub>3</sub> Si <sub>2</sub> U <sub>2</sub> Mo <sub>3</sub> Si <sub>4</sub>	I4/mcm P4/mbm P2 <sub>1</sub> /c	W <sub>5</sub> Si <sub>3</sub> U <sub>3</sub> Si <sub>2</sub> U <sub>2</sub> Mo <sub>3</sub> Si <sub>4</sub>	1.06942(1) 0.73279(1) 0.6883(1) <sup>c</sup>	0.53240(1) 0.38947(1) 0.6796(1)		49.8 59.4 23.3	12.9 0.1 32.5	37.3 40.5 44.2	
50	16.6	as-cast	U <sub>3</sub> Si <sub>2</sub> U <sub>2</sub> Mo <sub>3</sub> Si <sub>4</sub> Fine eutectic structure	P4/mbm P2 <sub>1</sub> /c	U <sub>3</sub> Si <sub>2</sub> U <sub>2</sub> Mo <sub>3</sub> Si <sub>4</sub>	1.07100(5)	0.53365(3)		58.4 22.7	1.0 33.2	40.6 44.1	
		850°C	U <sub>4</sub> Mo(Mo <sub>1-x</sub> Si <sub>x</sub> ) <sub>2</sub> Fine eutectic structure	I4/mcm	W <sub>5</sub> Si <sub>3</sub>				80.8 49.3	8.5 16.6	10.7 34.1	
50	19 <sup>a</sup>	as-cast	U <sub>4</sub> Mo(Mo <sub>1-x</sub> Si <sub>x</sub> ) <sub>2</sub> U <sub>2</sub> Mo <sub>3</sub> Si <sub>4</sub>	I4/mcm P2 <sub>1</sub> /c	W <sub>5</sub> Si <sub>3</sub> U <sub>2</sub> Mo <sub>3</sub> Si <sub>4</sub>				50.0 24.8	15.2 33.2	34.8 42.0	
		850°C	U <sub>4</sub> Mo(Mo <sub>1-x</sub> Si <sub>x</sub> ) <sub>2</sub> U <sub>2</sub> Mo <sub>3</sub> Si <sub>4</sub>	I4/mcm P2 <sub>1</sub> /c	W <sub>5</sub> Si <sub>3</sub> U <sub>2</sub> Mo <sub>3</sub> Si <sub>4</sub>				50.2 24.6	14.5 33.0	35.3 42.4	
50	27	850°C	U <sub>4</sub> Mo(Mo <sub>1-x</sub> Si <sub>x</sub> ) <sub>2</sub> γ-(U <sub>1</sub> Mo) U <sub>2</sub> Mo <sub>3</sub> Si <sub>4</sub>	I4/mcm Im $\bar{3}$ m P2 <sub>1</sub> /c	W <sub>5</sub> Si <sub>3</sub> W U <sub>2</sub> Mo <sub>3</sub> Si <sub>4</sub>				50.5 74.2 23.8	17.6 25.5 33.8	31.9 0.3 42.4	
72	5 <sup>a</sup>	850°C	U <sub>4</sub> Mo(Mo <sub>1-x</sub> Si <sub>x</sub> ) <sub>2</sub> U <sub>3</sub> Si	I4/mcm	W <sub>5</sub> Si <sub>3</sub>				50.7 75.5	13.4 0.2	35.9 24.3	
10	62	850°C	Mo <sub>3</sub> Si Mo <sub>5</sub> Si <sub>3</sub> U(Mo <sub>1-x</sub> Si <sub>x</sub> ) <sub>2</sub>	Pm $\bar{3}$ n I4/mcm P6 <sub>3</sub> /mmc	Cr <sub>3</sub> Si W <sub>5</sub> Si <sub>3</sub> MgZn <sub>2</sub>	0.48875(4) 0.96429(27) 0.53577(11)	– 0.49290(7) 0.85861(32)		0.3 0.1 33.6	75.5 63.8 43.9	24.2 36.1 22.4	

<sup>a</sup> Alloy contains small amounts of γ-(U<sub>1</sub>Mo). <sup>b</sup> Alloy contains small amounts of γ-(U<sub>1</sub>Mo) and (Mo). <sup>c</sup> b = 0.6878(1) and β = 109.9°.

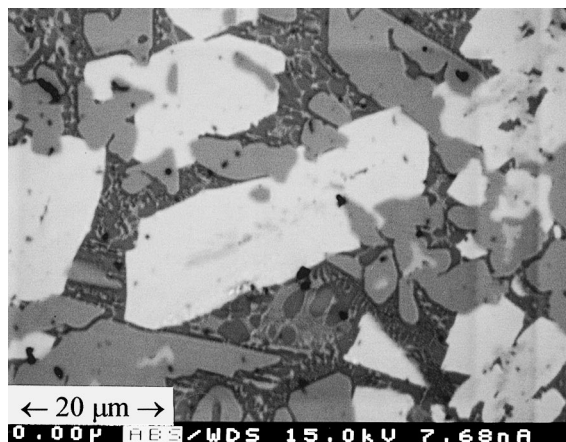


Fig. 2. As-cast alloy  $U_{50}Mo_{17}Si_{33}$  ( $'U_3MoSi_2'$ ), EMPA-absorption image. Large bright precipitates are  $U_2Mo_3Si_4$ , large gray grains are  $U_3Si_2$ , U-rich eutectic matrix with dark U-rich constituents.

Whereas the as-cast alloy  $U_4Mo_{1.3}Si_{2.7}$  essentially consists of  $U_2Mo_3Si_4$  ( $U_{22.7}Mo_{33.2}Si_{44.1}$ ) and  $U_3Si_2$  ( $U_{58.4}Mo_{1.0}Si_{40.6}$ ) with dark uranium-rich grains in the matrix ( $U_{\sim 90}Mo_{\sim 10}Si_{\sim 0.1}$ , see Fig. 2), after long-term anneal at  $850^\circ C$  the alloy was practically single-phase  $U_4Mo_{1.3}Si_{2.7}$  ( $U_{49.3}Mo_{16.6}Si_{34.1}$ ). Despite fine-grained matrix structures were formed in the alloys of  $U_{50}Mo_{19}Si_{31}$  and  $U_{50}Mo_{27}Si_{23}$ , a three-phase equilibrium is clearly revealed by EMPA:  $U_4Mo_{1.3}Si_{2.7} + U_2Mo_3Si_4$  ( $U_{23.8}Mo_{33.8}Si_{42.4}$ ) +  $\gamma$ -(U,Mo) ( $U_{74.2}Mo_{25.5}Si_{10.3}$ ). In this context it is interesting to mention, that  $\gamma$ -(U,Mo) was easily retained to room temperature in ternary alloys quenched from  $850^\circ C$ , although the  $\gamma$ -solid solution

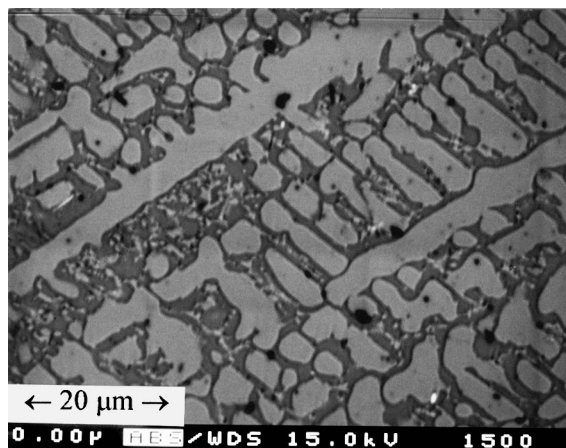


Fig. 3. Sample  $U_{72}Mo_5Si_{23}$ , as-cast alloy, EMPA-absorption image. Large bright dendrites are  $U_3Si_2$  ( $U_{60.1}Mo_{0.1}Si_{39.5}$ ) with matrix containing dark uranium-rich constituents (area scan:  $U \cong 82Mo \cong 8Si \cong 10$ ).

is metastable below about  $550^\circ C$  in the U–Mo binary [18].

As seen from the EMPA data of alloy  $U_{72}Mo_5Si_{23}$  (Fig. 3), there is practically no solid solubility at  $850^\circ C$  of Mo neither in  $U_3Si_2$  nor in  $U_3Si$  and there is virtually no solid solubility for Si in the (U,Mo)-binary. The low Mo-solubility in  $U_3Si_2$  of less than  $\cong 0.5$  at.% Mo is in good agreement with the findings of Ugajin [9,10], who reported 0.1 mass% Mo ( $\cong 0.16$  at.% Mo). Even in as-cast alloys the solubility of Mo in  $U_3Si_2$  is less than  $\cong 1.6$  at.% ( $U_{57.6}Mo_{1.6}Si_{40.8}$ ) with Mo replacing uranium atoms.

Two alloys were used to check on the formation and possible extent of the ternary Laves phase at  $850^\circ C$ :  $U_{33}Mo_{37}Si_{30}$  and  $U_{33}Mo_{56}Si_{11}$ . The existence of the Laves phase is confirmed from the microstructures and EMP analyses of both alloys, however, its region of existence is rather restricted at  $850^\circ C$  ranging from  $U(Mo_{0.67}Si_{0.33})_2$  to  $U(Mo_{0.7}Si_{0.3})_2$ . Whereas the Si-rich end of the phase ties to  $U_2Mo_3Si_4 + \gamma$ -(U,Mo), its Si-poor end is engaged in a three-phase equilibrium with  $\gamma$ -(U,Mo) (at  $U_{61.8}Mo_{38.1}Si_{0.1}$ ) and almost pure Mo ( $U_{1.5}Mo_{97.7}Si_{0.8}$ ) in form of a fine dendrite structure (Fig. 4).

From the present investigation of the phase equilibria it may safely be concluded that the phases  $'U_4MoSi_3'$  and  $'U_3MoSi_2'$ , reported to be individual compounds [9,10], are both part of a single-phase region  $U_4Mo(Mo_xSi_{1-x})_1Si_2$  with an extended homogeneous range,  $0 < x < 0.33$  (for structural formula see Section 3.3.2). Alloys with Si-rich compositions even after prolonged heat treatment revealed incomplete equilibrium conditions, phase relations based on the  $1400^\circ C$  section, however, are most probable. Based on these experimental findings, the phase partitioning, established at

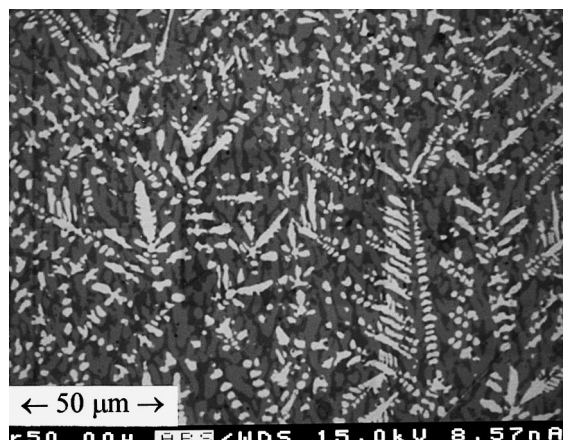


Fig. 4. Sample  $U_{33}Mo_{56}Si_{11}$ , annealed at  $850^\circ C$ , EMPA-absorption image. Large bright dendrites are Mo(U); gray particles are  $U(Mo_{1-x}Si_x)_2$ . Dark uranium-rich matrix is  $\gamma$ -(U,Mo) (at  $U_{64.3}Mo_{35.6}Si_{0.1}$ ).

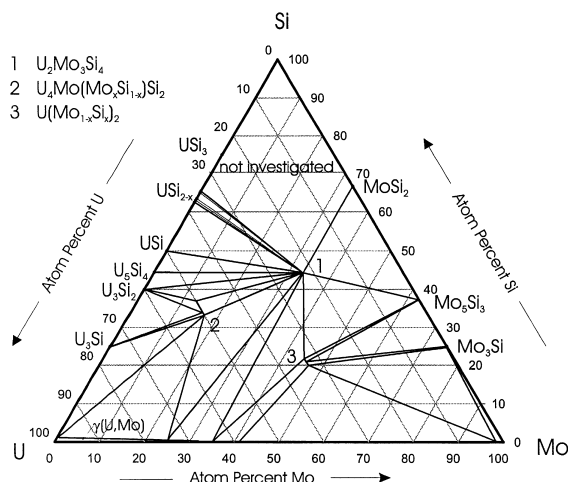


Fig. 5. Partial isothermal section at 850°C for the Mo–Si–U system for Si-compositions less than 50 at.%.

850°C in the Si-poor region below about 50 at.% Si, is shown in Fig. 5. Due to the formation of the ternary phases  $U_3MoSi_2$  and  $U(Mo_{0.67}Si_{0.33})_2$  within the join  $U_3Si_2$ –Mo, there is no thermodynamic equilibrium between  $U_3Si_2$  and (Mo). Furthermore the observed two-phase equilibria,  $U_2Mo_3Si_4 + \gamma(U,Mo)$ ,  $U(Mo_{0.67}Si_{0.33})_2 + \gamma(U,Mo)$  and  $U_4Mo(Mo_{1-x}Si_x)_3 + \gamma(U,Mo)$ , exclude thermodynamic compatibility between  $U_3Si_2$  and (Mo).

### 3.3. Structural chemistry

#### 3.3.1. The solid solution $U(Mo_{1-x}Si_x)_2$ with $MgZn_2$ -type

The authors of Ref. [7] proved isotypism of  $U(Mo_{0.625}Si_{0.375})_2$  with crystal symmetry and structure type of  $MgZn_2$  from a refinement of X-ray single-crystal intensity data. The refinement furthermore revealed a partial order among Mo and Si atoms. As seen from the isothermal section at 1400°C (Fig. 1), the ternary phase  $U(Mo_{1-x}Si_x)_2$  comprises a large homogeneous field,  $0.25 < x < 0.375$ , including the composition  $U(Mo_{0.75}Si_{0.25})_2$ , for which a full atom order could be expected. Evaluation of the X-ray intensity data, however, is incompatible with full atom order and merely yields preferential occupation of Mo-atoms in the sites (6h) of space group  $P6_3/mmc$ . At 850°C the homogeneity region appears substantially reduced to a mere width of about 2 at.% around the composition  $U(Mo_{0.68}Si_{0.32})_2$  (see Fig. 5). Quantitative Rietveld analysis of the X-ray intensity data of the alloy  $U(Mo_{0.68}Si_{0.32})_2$  again proved a high degree of statistical disorder in the Mo/Si sublattice but with a higher preference of Mo-atoms for the (6h) site than for the (2a) site. Table 3 documents the results of the Rietveld refinement ( $R_F = 0.049$ ) including interatomic distances, which reflect the tight atom bonding as typical for intermetallic clusters in Laves

phases. U–U distances,  $0.3204 < U-U < 0.3286$  nm, are rather short and indicate strong 5f–5f orbital overlap, which may in fact be responsible for the absence of magnetic order even at low-temperatures (see also Ref. [7] for magnetic data on  $U(Mo_{0.625}Si_{0.375})_2$ ).

The variation of unit cell dimensions throughout the homogeneity region as a function of Mo/Si atom exchange at constant U-content reflects the volume contraction due to the smaller size of the Si atom ( $R_{Si} = 0.134$ ;  $R_{Mo} = 0.140$  nm [21]). It is interesting to note, that the complicated nonlinear Mo/Si exchange within the two sublattices (6h) and (2a) reveals a minimum in the a-parameter for  $U(Mo_{0.68}Si_{0.32})_2$ , whilst the c-parameter shows a rather continuous decrease with increasing Si-content.

#### 3.3.2. The solid solution $U_4Mo(Mo_xSi_{1-x})Si_2$ with $W_5Si_3$ -type

The evaluation of X-ray powder patterns obtained from alloys annealed at 850°C in the region bound by the phases  $U - U_3Si_2 - U_2Mo_3Si_4 - U(Mo_{0.68}Si_{0.32})_2$  showed the formation of a ternary phase with a large region of existence. In combination with EMPA data the solid solution was found with a constant U-content of 50 at.% and to extend from 12 to 17 at.% Mo. The solid solution interestingly comprises the compositions of both compounds reported by Ugajin [9,10], ‘ $U_4MoSi_3$ ’ and ‘ $U_3MoSi_2$ ’. A comparison of the X-ray powder pattern reported by Ugajin [10] for ‘ $U_3MoSi_2$ ’ with the one we obtained for the corresponding composition leaves no doubt about the identity of the two phases. Employing the TREOR software [22], we were able to successfully index the Guinier X-ray pattern of our alloy  $U_3MoSi_2$  on the basis of a tetragonal unit cell with the parameters  $a = b = 1.0710$  and  $c = 0.5336$  nm. The  $a, b$ -parameters deduced are strikingly close to the value  $a = 1.069(1)$  obtained by Ugajin [10] from a tentative indexing on the basis of a cubic lattice. Applying the TREOR software on the X-ray data supplied in the paper by Ugajin [10], we successfully indexed all his data on the basis of a tetragonal cell ( $a = b = 1.0709$ ,  $c = 0.5336$  nm), which perfectly corresponds to the one received from our alloy. The size of the unit cell in combination with the X-ray intensities observed and the composition of the phase indicate a close resemblance with the  $W_5Si_3$ -type of structure. The Rietveld refinement of the X-ray data for  $U_4MoSi_3$  indeed converged at a convincingly low-residual value  $R_F = 0.029$ , proving isotypism with the structure type of  $W_5Si_3$ . A similar refinement of the intensity pattern for  $U_3MoSi_2$  confirmed the  $W_5Si_3$ -type. Full-matrix least-squares refinement of X-ray single-crystal intensity ( $F^2$ ) data (from Nonius Kappa CCD) of a single crystal broken from the alloy  $U_3MoSi_2$  and annealed at 1150°C, confirmed unit cell, crystal symmetry and isotypism with the structure type of  $W_5Si_3$ . The crystallographic data resulting from

Table 3  
Parameters of structure refinement<sup>a</sup> and interatomic distances for alloys  $U_4Mo_1Si_3$ ,  $U_3MoSi_2$  ( $W_5Si_3$ -type) and  $U(Mo_{0.73}Si_{0.27})_2$  ( $M_9Zn_2$ -type)

Parameter/compound/ nominal composition (at.%)	$U_4MoSi_3$ $U_{50}Mo_{12.5}Si_{37.5}$	$U_4Mo(Mo_xSi_{1-x})Si_3$ $U_{50}Mo_{16.7}Si_{33.3}$	$U(Mo_{1-x}Si_x)_2$ ; $x = 0.27$ $U_{33}Mo_{49}Si_{18}$
$a$ (nm)	1.069422(12)	1.07127(4)	0.53639(1)
$c$ (nm)	0.532400(8)	0.53391(2)	0.86045(2)
Space group; $Z$	14/mcm; origin at $\bar{1}$ ;	14/mcm; origin at $\bar{1}$ ;	$P6_3/mmc$ ; orig. at $\bar{1}$ ;
Structure type	$Z = 4$ ; ordered $W_5Si_3$ -type	$Z = 4$ ; $W_5Si_3$ -type	$Z = 4$ ; $MgZn_2$ -type
Density, $\rho_{exp}$ , $\rho_X$ ( $Mg\ m^{-3}$ )	$\rho_X = 12.35$	$\rho_{exp} = 12.1$ ; $\rho_X = 12.27$	$\rho_X = 12.18$
Data collection; X-rays	Powder data from Guinier Image plate; CuK $\alpha$	Single-crystal data from Nomius Kappa CCD; MoK $\alpha$	Powder data from Guinier Image plate; CuK $\alpha$
$2\Theta$ -range ( $^\circ$ )	8 to 110	5.38 to 90.66	8 to 110
Number of variables	35	18	28
Reflections in refinement	98	728(629 > $2\sigma$ ) (meas.12607)	59
$R_F = \sum  F_o - F_c  / \sum F_o$	0.029	–	0.049
$R_I = \sum  I_o - I_c  / \sum I_o$	0.044	–	0.069
$R_{wp} = [\sum w_i  y_{oi} - y_{ci} ^2 / \sum w_i y_{oi}^2]^{1/2}$	0.93	0.052 ( $> 2\sigma$ )	0.083
$R_P = \sum  y_{oi} - y_{ci}  / \sum  y_{oi} $	0.064	$R_w = 0.134$	0.066
$R_c = (N - P + C) / (\sum w_i  y_{oi} ^2)^{1/2}$	0.019	Overall $R_{merge} = 0.143$	0.029
$\chi^2 = (R_{wp}/R_c)^2$	22.5	GOF = 1.080	7.9
Atom parameters			
$B_{eq}(B_{iso})(nm^2)$	16 U1 in 16k ( $x, y, 0$ ) (0.09264(6), 0.22754(6), 0) 0.0024(2)	16 U1 in 16k ( $x, y, 0$ ) (0.0926(1), 0.2285(1), 0) 0.0079(1) <sup>b</sup>	4 U1 in 4f (1/3, 2/3, $z$ ) $z = 0.56381(5)$ 0.0028(9)
$B_{eq}(B_{iso})(nm^2)$ occupation	Mo in 4b (0, 1/2, 1/4) 0.0025(8) –	4 Mo1 in 4b (0, 1/2, 1/4) 0.0071(1) <sup>b</sup> –	M1 in 6h ( $x, 2x, 1/4$ ) $x = 0.1685(2)$ 0.0044(9) 4.60(1) Mo1 + 1.40 Si1
	8 Si1 in 8h ( $x, x + 1/2, 0$ ) $x = 0.1448(5)$	8 Si1 in 8h ( $x, x + 1/2, 0$ ) $x = 0.1466(3)$	M2 in 2a (0, 0, 0) 1.11(1) Mo2 + 0.89Si2

$B_{\text{eq}}(B_{\text{iso}})(\text{nm}^2)$ occupation	0.018(2)	0.0079(4) <sup>b</sup>	0.0045(9)
$B_{\text{eq}}(B_{\text{iso}})10^2(\text{nm}^2)$ occupation	–	–	–
Distances (nm) within the first nearest neighbor coordination; standard deviations are <0.00006 nm	–	–	–
	4 Si2 in 4a (0, 0, 1/4) 0.018(2)	4 M1 in 4a (0, 0, 1/4) 0.0110(1) <sup>b</sup> 1.12(1)Mo2 + 2.88Si2	
	–	–	–
	U1	U1	U1
	1U1 0.27196	1U1 0.27243	3Mo1 0.31040
	1Si1 0.28830	1Si1 0.28880	6Mo1 0.31240
	2Si2 0.29439	2Si2 0.29510	3Si2 0.31452
	1Si1 0.29452	1Si1 0.29490	1U 0.32041
	2Si1 0.30432	2Si1 0.30510	CN = 16
	2U1 0.33185	2U1 0.33266	3U 0.32857
	2Mo 0.33531	2Mo 0.33594	
	2U1 0.33539	2U1 0.33621	
	2U1 0.37156	2U1 0.37220	
	CN = 15	CN = 15	
	Mo	Mo	Mo1
	4Si1 0.25628	4Si1 0.25680	2Mo1 0.26516
	2Mo 0.26620	2Mo 0.26696	2Si2 0.26607
	CN = 14	CN = 14	2 Mo1 0.27123
	Si1	Si12	2U 0.31040
	2Mo 0.25628	Mo 0.25680	CN = 12
	2U1 0.28830	2U1 0.28880	4U 0.31240
	2U1 0.29439	2U1 0.29490	Si2 6Mo1 0.26607
	CN = 10	CN = 10	CN = 12
	4U1 0.30432	4U1 0.30510	6U 0.31452
	Si2	Si2	
	2Si1 0.26620	2Si1 0.26696	
	CN = 10	CN = 10	
	8U1 0.29452	8U1 0.29510	
Secondary phases	U <sub>3</sub> Si <sub>2</sub> ; U <sub>2</sub> Mo <sub>3</sub> Si <sub>4</sub>	(Mo); (U,Mo)	

<sup>a</sup> Crystal structure data were standardized using Program Typix [23].  
<sup>b</sup> Anisotropic displacement factors (nm<sup>2</sup>) are: U1 : U<sub>11</sub> = U<sub>22</sub> = 0.00010(1); U<sub>33</sub> = 0.00012(1); Mo1 : U<sub>11</sub> = U<sub>22</sub> = 0.00009(1); U<sub>33</sub> = 0.00009(1); Si1 : U<sub>11</sub> = U<sub>22</sub> = 0.00009(1); U<sub>33</sub> = 0.00012(2); M1 : U<sub>11</sub> = U<sub>22</sub> = 0.00014(1); U<sub>33</sub> = 0.00014(2).



Table 4

Crystallographic data of the ternary compounds in the system U–Mo–Si, and comparison with data in literature

Compound	Lattice parameters (nm)				Comments	Reference
	<i>a</i>	<i>b</i>	<i>c</i>	$\beta$ (°)		
U <sub>2</sub> Mo <sub>3</sub> Si <sub>4</sub>	0.6876(3)	0.6883(1)	0.6760(3)	109.79(2)	annealed at 1400°C	[8,24]
	0.6877	0.6884	0.6765	109.9		[5]
U(Mo <sub>1-x</sub> Si <sub>x</sub> ) <sub>2</sub>	0.53730(5)	0.53730(5)	0.85334(9)	–	at <i>x</i> = 0.375, 1400°C; Mo-poor	This work
	0.53735(7)	0.53735(7)	0.85958(19)	–	at <i>x</i> = 0.250, 1400°C; Mo-rich	This work
	0.53670(10)	0.53670(10)	0.85901(18)	–	at <i>x</i> = 0.33, 850°C; Mo-poor	This work
	0.53663(4)	0.53663(4)	0.85417(19)	–	at <i>x</i> = 0.30, 850°C; Mo-rich	This work
	0.53729(4)	0.53729(4)	0.8527(2)	–	at <i>x</i> = 0.375	[7]
	0.5370	0.5370	0.8582	–	at <i>x</i> = 0.375	[6]
U <sub>4</sub> Mo(Mo <sub>x</sub> Si <sub>1-x</sub> )Si <sub>2</sub>	1.06944(1)	1.06944(1)	0.53238(1)	–	at <i>x</i> = 0.0, 850°C	This work
	1.07100(5)	1.07100(5)	0.53365(3)	–	at <i>x</i> = 0.33, 850°C	This work

the various refinements and including interatomic distances are summarised in Table 3. A calculation of the X-ray density for U<sub>3</sub>MoSi<sub>2</sub>,  $\rho_X = 12.27 \text{ Mg m}^{-3}$ , is in close agreement with the experimentally observed value of  $12.1 \text{ Mg m}^{-3}$ , as reported by Ugajin [10]. Interatomic distances reveal tight bonding in the Mo/Si clusters but with a rather wide spread of U–U contacts,  $0.272 < \text{U–U} < 0.371 \text{ nm}$ . The extremely short bonds, U–U = 0.272 nm, ranking among the shortest known contacts in uranium intermetallics (U–U = 0.278 nm in U<sub>2</sub>Ti; U–U = 0.284 nm in U(Co, Si)<sub>2</sub>, etc.), imply a high degree of 5f–5f orbital overlap in favour of non-magnetic uranium–uranium interactions (see also Section 4, ‘magnetism’).

The results of EMP and X-ray diffraction analyses thus invoke a continuous solid solution with the W<sub>5</sub>Si<sub>3</sub>-type extending at 850°C from U<sub>4</sub>MoSi<sub>3</sub> to U<sub>3</sub>MoSi<sub>2</sub> as isotypic end members of the homogeneity region. X-ray refinements furthermore provide the atom site occupation scheme yielding full atom order for U<sub>4</sub>MoSi<sub>3</sub> and partial atom order for U<sub>3</sub>MoSi<sub>2</sub> with a statistical Mo/Si occupation of only the (4a) sites of space group I4/mcm (U<sub>4</sub>Mo(Mo<sub>0.33</sub>Si<sub>0.67</sub>)<sub>1</sub>Si<sub>2</sub> ≡ U<sub>3</sub>MoSi<sub>2</sub>). A proper structural chemical formula for the solid solution is then U<sub>4</sub>Mo(Mo<sub>x</sub>Si<sub>1-x</sub>)<sub>1</sub>Si<sub>2</sub>,  $0 < x < 0.33$ . U<sub>4</sub>MoSi<sub>3</sub> and U<sub>3</sub>MoSi<sub>2</sub> being isotypic end members of a continuous solid solution therefore, cannot both participate in an isothermal ternary four-phase reaction as proposed by Ugajin [10] for the peritectic formation of U<sub>3</sub>MoSi<sub>2</sub> at  $(1480 \pm 30)^\circ\text{C}$ . Although we confirm the peritectic mode of formation for the phase U<sub>4</sub>Mo(Mo<sub>x</sub>Si<sub>1-x</sub>)<sub>1</sub>Si<sub>2</sub>, we notice the primary precipitation of U<sub>3</sub>Si<sub>2</sub> in the microstructures of both as-cast alloys, U<sub>4</sub>MoSi<sub>3</sub> and U<sub>3</sub>MoSi<sub>2</sub>. Therefore, the peritectic formation of the phase U<sub>4</sub>Mo(Mo<sub>x</sub>Si<sub>1-x</sub>)<sub>1</sub>Si<sub>2</sub> may proceed according to the reaction:  $\text{L} + \text{U}_3\text{Si}_2 + \text{U}_2\text{Mo}_3\text{Si}_4 \rightleftharpoons \text{U}_4\text{Mo}(\text{Mo}_x\text{Si}_{1-x})_1\text{Si}_2$ . The value of *x* for the phase formed in the peritectic reaction is still not determined precisely enough. So is the peritectic liquid for which Ugajin [10]

reported a composition of U<sub>74</sub>Mo<sub>16</sub>Si<sub>10</sub>, a value rather low in Mo, when compared to the composition of the eutectic microstructure U<sub>76</sub>Mo<sub>10</sub>Si<sub>14</sub>, obtained by an area-scan of eutectic islands in the as-cast alloy U<sub>4</sub>MoSi<sub>3</sub> (see Table 2).

#### 4. Magnetism

The magnetism has been investigated for U<sub>2</sub>Mo<sub>3</sub>Si<sub>4</sub> [8,25] and for U(Mo<sub>0.625</sub>Si<sub>0.375</sub>)<sub>2</sub> [7]. In agreement with these data we find that U<sub>2</sub>Mo<sub>3</sub>Si<sub>4</sub> is weakly paramagnetic above 50 K with  $\mu_{\text{eff}} = 2.30 \mu_{\text{B}}/\text{U-atom}$ ,  $\Theta_{\text{p}} = -240 \text{ K}$  and  $\chi_0 = 1.4 \times 10^{-3} \text{ emu/mol}$  ( $1.7 \times 10^{-8} \text{ m}^3/\text{mol}$ ). It is temperature independent paramagnetic below 30 K. U(Mo<sub>0.62</sub>Si<sub>0.38</sub>)<sub>2</sub> proved to be temperature independent paramagnetic between 5 and 300 K with  $\chi_0 = 4.3 \times 10^{-3} \text{ emu/mol}$  ( $5.4 \times 10^{-8} \text{ m}^3/\text{mol}$ ). U<sub>4</sub>(Mo<sub>0.33</sub>–Si<sub>0.67</sub>)<sub>1</sub>Si<sub>2</sub> is practically temperature independent paramagnetic with  $\chi_0 = 2.7 \times 10^{-3} \text{ emu/mol}$  ( $3.4 \times 10^{-8} \text{ m}^3/\text{mol}$ ). Below 180 K, a slight increase of the susceptibility is observed, which cannot be attributed with certainty to an intrinsic behaviour.

#### 5. Summary

Phase equilibria in the ternary system Mo–Si–U have been established in an isothermal section at 1400°C for the region with less than 70 at.% U and at 850°C for the Si-poor region Mo–Mo<sub>5</sub>Si<sub>3</sub>–U<sub>2</sub>Mo<sub>3</sub>Si<sub>4</sub>–USi–U. From the three ternary compounds observed and characterised by means of refinement of X-ray powder or single-crystal intensity data we confirm existence and structure of stoichiometric U<sub>2</sub>Mo<sub>3</sub>Si<sub>4</sub> (U<sub>2</sub>Mo<sub>3</sub>Si<sub>4</sub>-type), as well as of the ternary MgZn<sub>2</sub>-type Laves phase U(Mo<sub>1-x</sub>Si<sub>x</sub>)<sub>2</sub> for which we determined the homogeneous region extending at 1400°C from U(Mo<sub>0.62</sub>Si<sub>0.38</sub>)<sub>2</sub> to U(Mo<sub>0.75</sub>Si<sub>0.25</sub>)<sub>2</sub> but with a rather small field of existence at 850°C around the

composition  $U(\text{Mo}_{0.68}\text{Si}_{0.32})_2 \cdot U_4\text{Mo}(\text{Mo}_x - \text{Si}_{1-x})_1\text{Si}_2$  is a novel ternary compound extending at (see Table 4) 850°C from  $x = 0$  to  $x = 0.33$  with an ordered structure variant of the  $W_5\text{Si}_3$ -type. The homogeneity region comprises both compositions  $U_4\text{MoSi}_3$  and  $U_3\text{MoSi}_2$  claimed earlier in the literature as individual ternary compounds. Whilst a high degree of statistical disorder is observed for all compositions within the homogeneity region of the Laves phase, the  $W_5\text{Si}_3$ -type phase comprises a fully ordered structure at  $x = 0$  and random occupation of Mo/Si atoms in only the (4a)-sites of space group I4/mcm for  $x = 0.33$ .

The short U–U distances determined for all the structures investigated are in perfect agreement with the experimentally observed temperature independent paramagnetic behaviour.

### Acknowledgements

This research was in part sponsored (T. LeBihan) by the European Union as a Human Capital and Mobility Network ERBCHRXCT930284. P.R. wishes to thank the Austrian National Science Foundation (Fonds zur Förderung der Wissenschaftlichen Forschung in Österreich) for support under grant P8218. The authors are furthermore grateful to the French–Austrian exchange programme PICS-134 between CNRS and the Austrian Academy of Sciences. Expertised assistance in the EMPA-XMA-measurements is due to M. Bohn from CNRS-URA 1278, IFREMER, Brest, France.

### References

- [1] F. Weitzer, M. Potel, H. Noël, P. Rogl, J. Solid State Chem. 111 (1994) 267.
- [2] T. LeBihan, H. Noël, P. Rogl, J. Alloys Compounds 213&214 (1994) 540.
- [3] A. Zelinsky, Y.N. Grin, K. Hiebl, P. Rogl, H. Noël, G. Hilscher, G. Schaudy, J. Magn. Magn. Mater. 139 (1995) 23.
- [4] T. LeBihan, H. Noël, P. Rogl, J. Nucl. Mater. 277 (2000) 82.
- [5] M. Sikirica, L.G. Akselrud, Y.P. Yarmolyuk, The Crystal Structure of the Compound  $U_2\text{Mo}_3\text{Si}_4$ , Abstracts of the third All Union Conference on the Crystal Chemistry of Intermetallic Compounds, Vyshcha Shkola, L'viv, (1978) 11 (in Russian).
- [6] M. Sikirica, Z. Ban, New Nuclear Materials Including Non-metallic Fuels, Proceedings, Prague 2 (1963) 229.
- [7] T. LeBihan, J.C. Levet, H. Noël, J. Solid State Chem. 121 (1996) 479.
- [8] T. LeBihan, H. Noël, J. Alloys Compounds 227 (1995) 44.
- [9] M. Ugajin, A. Itoh, J. Alloys Compounds 213&214 (1994) 369.
- [10] M. Ugajin, A. Itoh, S. Okayasu, Y. Kazumata, J. Nucl. Mater. 257 (1998) 145.
- [11] J.A. Straatmann, N.F. Neumann, Equilibrium Structures in the High Uranium–Silicon Alloy System, USAEC Report MCW1486, Mallinckrodt Chemical Works, 23 October, 1964, cited in Reactor Mater. 8(2) (1965) 57.
- [12] U.S. Nuclear Regulatory Commission Report, NUREG-1313, July 1988.
- [13] J. Rodriguez-Carvajal, FULLPROF: a program for Rietveld refinement and pattern matching analysis, Abstracts of the Satellite Meeting on Powder Diffraction of the XV Congress of the International Union of Crystallogr., Toulouse, France, 1990.
- [14] K. Remschnig, T. LeBihan, H. Noël, P. Rogl, J. Solid State Chem. 97 (1992) 391.
- [15] Nonius Kappa CCD Program Package COLLECT, DENZO, SCALEPACK, SORTAV, Nonius BV, Delft, The Netherlands, 1998.
- [16] G.M. Sheldrick, SHELXS-97; Program for Crystal Structure Determination, Univ. Göttingen, Germany, 1997; Windows version by P. McArdle, National University, Ireland, Galway.
- [17] L. Pouchou, F. Pichoir, J. Microsc. Spectrosc. Electron. 10 (1985) 279.
- [18] B.T. Massalski, Binary Alloy Phase Diagrams, 2nd Ed., ASM, Materials Park OH, USA, 1990.
- [19] P. Villars, L.D. Calvert, Pearson's Handbook of Crystallographic Data for Intermetallic Phases, 2nd Ed., ASM, Materials Park OH, USA, 1991.
- [20] V. Sechovsky, L. Havela, in: E.P. Wohlfahrt, K.H.J. Buschow (Eds.), Ferromagnetic Materials, Vol. 4, Elsevier, Amsterdam, 1988, p. 309.
- [21] E. Teatum, K. Gschneidner, J. Waber, Report LA-2345 (1960).
- [22] P.E. Werner, Program SCANPI8; Arrhenius Laboratory, Stockholm University, Sweden, 1990.
- [23] E. Parthé, L. Gelato, B. Chabot, M. Penzo, K. Cenzual, R. Gladyshevskii, Typix-standardized data and crystal chemical characterization of inorganic structure types, Gmelin Handbook of Inorganic and Organometallic Chemistry, 8th Ed., Vols. 1–4, Springer, Berlin, 1994.
- [24] F. Wastin, J. Rebizant, J.P. Sanchez, A. Blaise, J. Goffart, J.C. Spirlet, C.T. Walker, J. Fuger, J. Alloys Compounds 210 (1994) 83.
- [25] S.K. Patapis, J.C. Spirlet, J. Fuger, Solid State Commun. 98 (1996) 99.